Science of the Total Environment 724 (2020) 138291

Contents lists available at ScienceDirect

Science of the Total Environment

journal homepage: www.elsevier.com/locate/scitotenv

Probing extracellular reduction mechanisms of *Bacillus subtilis* and *Escherichia coli* with nitroaromatic compounds

Xinwei Zhou [a], Fuxing Kang [b], Xiaolei Qu [a], Heyun Fu [a], Juan Liu [c], Pedro J. Alvarez [d], Dongqiang Zhu [a,e,*]

[a] State Key Laboratory of Pollution Control and Resource Reuse, School of the Environment, Nanjing University, Jiangsu 210023, China
[b] College of Resources and Environmental Sciences, Nanjing Agricultural University, Jiangsu 210095, China
[c] School of Environmental Science and Engineering, Peking University, Beijing 100871, China
[d] Department of Civil and Environmental Engineering, Rice University, Houston, TX 77251, USA
[e] School of Urban and Environmental Sciences, Key Laboratory of the Ministry of Education for Earth Surface Processes, Peking University, Beijing 100871, China

HIGHLIGHTS

- Bacterial suspensions of *E. coli* or *B. subtilis* can readily reduce NACs.
- Reduction of NACs occurs predominantly within the extracellular matrix.
- Hemiacetal groups in EPS serve as the primary electron donor agents.
- Cytochromes, flavins and quinones in EPS serve as electron transfer mediators.
- Reduction of NACs is nonenzymatic and driven by extracellular electron transfer.

GRAPHICAL ABSTRACT

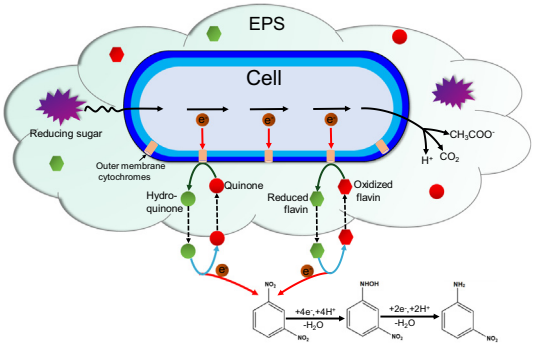

ARTICLE INFO

Article history:
Received 11 February 2020
Received in revised form 26 March 2020
Accepted 27 March 2020
Available online 28 March 2020

Editor: Fang Wang

Keywords:
Extracellular polymeric substances
Extracellular reduction
Extracellular electron transfer
Bacteria
Nitroaromatic compounds

ABSTRACT

Redox transformations of organic contaminants by bacterial extracellular polymeric substances (EPS) and the associated electron transfer mechanisms are rarely reported. Here we show that a nitroaromatic compound (1,3-dinitrobenzene) can be readily reduced to 3-hydroxylaminonitrobenzene and 3-nitroaniline in aqueous suspension of common bacteria (*E. coli* or *B. subtilis*) or in aqueous dissolved EPS extracted from the bacteria. The loss ratio of 1,3-dinitrobenzene by *E. coli* was unaffected after knocking out the *nfsA* gene encoding nitroreductase, but was suppressed by removing EPS attached to cells. In contrast, the loss ratio was enhanced by adding aqueous dissolved EPS to *E. coli* or *B. subtilis* suspension. The residual 1,3-dinitrobenzene and products formed after reduction were only presented outside the bacterial cells. Thus, bacterial reduction of 1,3-dinitrobenzene was mediated by nonenzymatic extracellular reduction. This was further corroborated by the observation that the stoichiometric demand of electrons in 1,3-dinitrobenzene reduction was nearly equal to the quantity of electrons donated by bacterial cells in the electrochemical cell experiment. Inhibition on the reduction of 1,3-dinitrobenzene by chemical probes combined with fluorescence detection demonstrated that reducing sugars in EPS might act as electron donors, while cytochromes and some low-molecular weight molecules (flavins and quinones) were involved as electron transfer mediators. Linear relationships were observed between the reduction kinetics and the one-electron reduction potentials for a series of substituted dinitrobenzenes in the presence of bacterial cells or dissolved EPS. Their close linear regression slope values suggest that the extracellular matrix and the exfoliated EPS utilized the same reducing agents (likely hydroquinones and reduced flavins) as terminal

* Corresponding author at: State Key Laboratory of Pollution Control and Resource Reuse, School of the Environment, Nanjing University, Jiangsu 210023, China.
E-mail address: zhud@pku.edu.cn (D. Zhu).

https://doi.org/10.1016/j.scitotenv.2020.138291

electron donors to reduce NACs. These results reveal a previously unrecognized mechanism for nonenzymatic extracellular reduction of NACs by common bacteria.
Capsule: The extracellular matrix of *E. coli* or *B. subtilis* supplies both electron donors and electron transfer mediators to efficiently reduce nitroaromatic compounds.

1. Introduction

Extracellular electron transfer (EET) is essential to material and energy exchange of microbial cells with the external environment (Gralnick and Newman, 2007; Lovley, 2008), and plays a pivotal role in microbial dissimilatory metal reduction (iron, manganese, chromium) (Shi et al., 2016), conversion of organic pollutants (e.g., azo dye decolorization and pentachlorophenol dehalogenation) (Pearce et al., 2010; Zhang and Katayama, 2012), and sustainable bioenergy applications (Lovley, 2006). Although many key details remain unresolved, EET is known to proceed via two general strategies: contact-dependent direct transfer through multiheme cytochromes (Carlson et al., 2012; Xiong et al., 2006) or nanowires (Reguera et al., 2006), and indirect transfer through dissolved redox-active electron-shuttling mediators that are produced by bacteria (e.g., flavins and quinones) (Light et al., 2018; Marsili et al., 2008; Newman and Kolter, 2000) or naturally present substances (humic quinone content) (Zhang and Katayama, 2012).

Microorganisms can secrete and surround themselves by extracellular polymeric substances (EPS) comprising a mixture of diverse types of biopolymers, mostly polysaccharides and proteins. EPS play a key role in cell surface attachment and microhabitat formation to offer resistance to desiccation, antibiotics, high salinity, and extreme temperature and pH conditions (Boggs et al., 2016; Flemming and Wingender, 2010; Vu et al., 2009). As a major component of biofilms (up to 90% of dry weight biomass), EPS are an important constituent of labile natural organic matter pool and contribute to biogeochemical cycles of organic matter and nutrient elements (Flemming and Wingender, 2010; Vu et al., 2009). Although EPS are known to keep many redox-active and/or electron-conductive components (e.g., proteins, flavins, and quinones) (Borole et al., 2011; Li et al., 2016; Xiao et al., 2017), it remains unclear how and to what extent EPS affect the extracellular redox-transformation of heavy metal ions and organic pollutants.

Nitroaromatic compounds (NACs) are widely used in many industries and agriculture as solvents, organic synthesis intermediates, explosives, and pesticides. Consequently, NACs are inevitably released into the environment, posing risks to environmental and public health due to their potential toxicity and carcinogenicity (Kulkarni and Chaudhari, 2007; Spain, 1995). Owing to the strong electron-withdrawing ability of the nitro group, the aromatic ring of NACs is electron deficient; therefore, direct oxidative attack by oxygenases from aerobic bacteria is rarely reported, particularly when the NACs are not substituted with electron-donating groups (amines and phenols) (Kulkarni and Chaudhari, 2007; Marvin-Sikkema and Bont, 1994; Spain, 1995). Alternatively, a variety of anaerobic microorganisms (e.g., Fe(III)- and sulfate-reducing bacteria) are reported to reduce NACs in the presence of electron-donor substrates (Gorontzy et al., 1993; Yuan et al., 1997). However, the underlying mechanisms associated with the reduction of nitro groups are not well understood. Nitroreductases (mostly *in vitro* and purified) are also known to catalyze the reduction of nitro groups in NACs to hydroxylamines or amines in the presence of electron donors (Roldán et al., 2010; Somerville et al., 1995), but there is insufficient evidence for their direct interaction with NACs *in vivo* (Roldán et al., 2010; Spain, 1995). Additionally, because most nitroreductases exist within cells, microorganisms that rely on nitroreductases to reduce NACs will have to be able to resist and/or tolerate the intermediates and products (such as hydroxylamino- and aminobenzene derivatives), which are often more toxic to microorganisms (Aruoja et al., 2011; Spain, 1995; Yuan et al., 1997).

To date only a few studies have reported extracellular reduction of organic contaminants (limited to pentachlorophenol and azo-dyes), which involves Gram-negative *Shewanella* sp. and *Geobacter* sp. under anaerobic conditions (Pearce et al., 2010; Zhang and Katayama, 2012). We previously reported that EPS extracted from a variety of pure-culture microorganisms (*Escherichia coli*, *Bacillus subtilis*, *Phanerochaete chrysosporium*, and *Saccharomyces cerevisiae*) and natural biofilm alone could reduce 1,3-dinitrobenzene to 3-hydroxylaminonitrobenzene and 3-nitroaniline (Kang and Zhu, 2013). Spectroscopic analyses of the EPS before and after reaction with 1,3-dinitrobenzene combined with Tollen's test suggested that the hemiacetal groups of rhamnose and some phenolic groups in EPS acted as the reducing agents. However, the role played by EPS on intact bacterial cells in NACs reduction remains unknown.

The main objective of this study is to discern how NACs could be reduced in the extracellular matrix of common bacteria (*Escherichia coli* and *Bacillus subtilis*) without exogenous electron-donor substrates. Using batch reaction experiments and an array of chemical, electrochemical, and biological analyses integrated with apparent kinetic isotope effect (AKIE), we determined the functional components in EPS (exfoliated from bacteria and in intact cells) responsible for NACs reduction, and elucidated the underlying mechanisms for the nonenzymatic extracellular reductive reaction.

2. Materials and methods

2.1. Materials

NACs including 1,3-dinitrobenzene (abbreviated to 1,3-DNB), 2,4-dinitrobenzoic acid (abbreviated to *o*-COOH as referenced by 1,3-DNB), 2,4-dinitrobenzaldehyde (*o*-CHO), 2,4-dinitrophenol (*o*-OH), 2,4-dinitrochlorobenzene (*o*-Cl), 2,4-dinitrotoluene (*o*-CH_3), 1,3,5-trinitrobenzene (*m*-NO_2), and 3-nitroaniline were purchased from Sigma-Aldrich (St. Louis, MO, USA) in the highest purity. Sodium azide (NaN_3) and chloroauric acid ($HAuCl_4$) were also purchased from Sigma-Aldrich. Sodium sulfide (Na_2S), rotenone, and riboflavin were from Sinopharm Chemical Reagent Co., Ltd. (China). Juglone was purchased from CNW Technologies GmbH (Germany). Ultrapure water (18.2 MΩ·cm) was produced by a Milli-Q system (Millipore, Bedford, MA). Peptone, yeast extract, and sodium chloride in biotechnology grade from Oxoid Co., Ltd. (England) were used to prepare Luria-Bertani (LB) medium containing 10 $g \cdot L^{-1}$ peptone, 5 $g \cdot L^{-1}$ yeast extract, and 10 $g \cdot L^{-1}$ NaCl.

2.2. Preparation of bacterial cell suspension and extraction of EPS

The tested bacterial strains were Gram-positive *Bacillus subtilis* (*B. subtilis*, GIM 1.372) and Gram-negative *Escherichia coli* DH5α (*E. coli*, GIM 1.571). The *E. coli* cells were further transformed commercially (Sangon Biotech Co., Ltd., Shanghai) by knocking out the *nfsA* gene encoding nitroreductase (NfsA) to obtain a new strain named Δ*nfsA*. The bacteria were cultured in 20 mL of LB medium at 37 °C for 12 h, then transferred into 1 L of fresh LB medium, and cultured for another 48 h to reach a stable phase. The bacteria were separated from LB medium by centrifugation (6000*g* at 4 °C for 10 min), followed by repeated

washing with Milli-Q water. The obtained cell pellets were resuspended with Milli-Q water (approximately 5×10^{12} cells·L^{-1}). The obtained cell suspension of *B. subtilis* or *E. coli* was used for the following extraction of dissolved EPS and kinetic experiments.

Preparation of dissolved EPS from *B. subtilis* and *E. coli* was performed using a chemical-free, sonication method as described in our previous study (Kang and Zhu, 2013). Briefly, cell suspension (6.7×10^{12}–1.0×10^{13} cells·L^{-1}) was sonicated with an intensity of 2.7 W·cm^2 and a frequency of 50 kHz at 4 °C for 15 min to separate EPS from bacterial cells, and then immediately centrifuged (10,000*g* at 4 °C for 20 min) for removing the cells. The supernatant was collected and filtered through a 0.22-μm membrane (Anpel). The obtained filtrate containing dissolved EPS (54.8 mgC·L^{-1} on the basis of total organic carbon/TOC) was stored at 4 °C for later use. Cell lysis during the EPS extraction was negligible as indicated by the very low nucleic acid concentration (Kang and Zhu, 2013; Kang et al., 2014). One portion of bulk *B. subtilis* EPS was further separated into two different molecular weight (MW) fractions by ultrafiltration using a Centricon-3 membrane with cutting off 3 kDa (Milipore, USA). The obtained low-MW EPS (MW < 3 kDa) and high-MW EPS (MW > 3 kDa) accounted for 65% and 31% of the TOC of bulk *B. subtilis* EPS.

2.3. Reduction of 1,3-DNB in the presence of bacteria or EPS

The reduction of 1,3-DNB in the presence of *B. subtilis* or *E. coli* cells was examined under three different EPS conditions: without manipulation of EPS (referred to as pristine cells), with removal of EPS using above sonication/centrifugation method (referred to as low-EPS cells), and with addition of dissolved EPS at 7.2 mgC·L^{-1} (referred to as high-EPS cells). To initiate the batch reaction experiments, methanol stock solution of 1,3-DNB (<0.1% in volume) was added to 65 mL of bacterial cell suspension containing 2×10^{12} cells·L^{-1} in 65-mL sterilized brown glass vials equipped with Teflon-lined butyl rubber stoppers. The initial concentration of 1,3-DNB was 30 μmol·L^{-1} for *B. subtilis* cells and 40 μmol·L^{-1} for *E. coli* cells. The samples were incubated and shaken by an orbital shaker in the dark at 35 ± 0.5 °C, and aliquots (<0.5 mL) were sampled at desired time intervals (0–10 h for *B. subtilis* cells and 0–3 h for *E. coli* cells). The collected aliquot was treated by the above-mentioned sonication/centrifugation method to facilitate the transfer of 1,3-DNB and its reaction product and intermediate sorbed on the bacterial surface into the aqueous phase. The supernatant was withdrawn and stored (referred to as extracellular samples). A separate analysis was performed to test the possibility of intracellular reduction of 1,3-DNB. After removal of EPS by sonication/centrifugation, pellets of *B. subtilis* cells at reaction times of 0, 5, and 10 h and *E. coli* cells at reaction times of 0, 1, and 3 h were resuspended with Milli-Q water and disrupted by high intensive focused ultrasound (HIFU) (Φ6, Scientz, China) with an intensity of 450 W·cm^2 and a frequency of 24 kHz at 0 °C for 5 min. After centrifugation (10,000*g* at 4 °C for 20 min), the supernatant containing cell lysate was collected and stored (referred to as intracellular samples). The obtained pellets of cell debris were extracted twice with methanol by orbital shaking for 20 min at room temperature, and the supernatant was collected and stored (referred to as cell debris samples). Triplicate samples were run for each time point in batch reaction experiments. The pH of bacterial suspensions was measured to be 6.8 ± 0.3 at the end of the batch reaction experiments.

The collected extracellular samples, intracellular samples, and cell debris samples were analyzed by a high-performance liquid chromatography (HPLC) equipped with a photodiode array detector (Model 1200, Agilent) using an XDB-C18 column (Agilent). Isocratic elution (55% acetonitrile/45% water, v/v) was run at 25 °C with a flow rate of 1.0 mL·min^{-1}. The detection wavelength was set at 245 nm for 1,3-DNB, 3-nitroaniline (product), and 3-hydroxylaminonitrobenzene (intermediate). Their concentrations were measured according to calibration curves prepared by corresponding standard compounds. Identifications of 3-nitroaniline and 3-hydroxylaminonitrobenzene were further verified by gas chromatography mass spectrometry (Trace DSQ, Thermo-Fisher, USA) analysis of the dichloromethane extract of the aliquot using a method as described in our previous study (Kang and Zhu, 2013).

Meanwhile, the kinetics of 1,3-DNB reduction in the presence of EPS extracted from *B. subtilis* or *E. coli* was examined by a similar set of experiments, except that the experiments were conducted in a glove box filled with high-purity nitrogen for eliminating oxygen. The EPS solution (54.8 mgC·L^{-1}) was also purged with nitrogen to remove dissolved oxygen prior to spiking of 1,3-DNB (initially at 13.0 μmol·L^{-1}). The fractionalized low-MW EPS and high-MW EPS from bulk *B. subtilis* EPS were also tested in 1,3-DNB reduction. Triplicate samples were run for each time point in batch reaction experiments. The pH of EPS solutions was measured to be 7.3 ± 0.2 at the end of the batch reaction experiments.

To further evaluate the potential role of redox and/or electron-transfer active substances in 1,3-DNB reduction by bacterial cells or EPS, suppression experiments were conducted in the presence of 9.2-mM sodium azide (a cytochrome inhibitor) (Yang, 1985) or 0.1-mM rotenone (a NADH-ubiquinone reductase inhibitor) (Esposti, 1998). Another set of experiments was run to assess the suppression effect of gold ion (Au^{3+}, 0.025 mM), a consumer of reducing agents such as hemiacetals (Kang et al., 2017), on 1,3-DNB reduction by EPS. This suppression experiment was not conducted on bacterial cells considering the cytotoxicity of Au^{3+} (Kang et al., 2017).

2.4. Spectroscopic measurements of electron transfer mediators

Electron transfer mediators (flavins and quinones) possibly involved in 1,3-DNB reduction were detected by fluorescence spectrophotometer (Hitachi F-4500). Prior to analysis, the bacterial cell suspension was centrifuged at 10,000*g* for 10 min at 4 °C to obtain the extracellular supernatant. The flavins in the extracellular supernatant, bulk EPS, low-MW EPS, and high-MW EPS were detected by scanning the fluorescence emission spectra (465–800 nm) at 464 nm excitation wavelength (Wang et al., 2013). The quinone derivatives in these samples were detected by scanning the fluorescence emission spectra (365–500 nm) at 350 nm excitation wavelength (Chen et al., 2003; Cory and Mcknight, 2005).

2.5. Structure activity relationship (SAR) for NACs reduction

The SAR was examined for cell suspension (2×10^{12} cells·L^{-1} for *B. subtilis* and 1.8×10^{12} cells·L^{-1} for *E. coli*) and dissolved EPS (28.4 mgC·L^{-1} for *B. subtilis* EPS and 30.3 mgC·L^{-1} for *E. coli* EPS) with a total of seven NACs, including 1,3-DNB, *o*-Cl, *o*-CHO, *o*-COO^-, *o*-O^-, *o*-CH_3, and *m*-NO_2. The SAR was assessed by linear regression on the logarithms of the observed pseudo-first-order kinetic rate constants (k_{obs}, h^{-1}) of the NACs versus their one-electron reduction potentials referenced with a standard hydrogen electrode (E^1_H, V). The gas-phase E^1_H values of NACs were calculated by density functional theory (DFT) with the 6-31+G(d,p) basis set and the B3LYP exchange correlation functions (Phillips et al., 2008). The aqueous-phase E^1_H values of NACs were then calculated by incorporating the respective gas-phase E^1_H values with the free energy changes associated with the solvation process, which were calculated using the COSMO-SMD continuum solvation model by the NWChem Software Suite (Salter-Blanc et al., 2015). The calculated aqueous-phase E^1_H values were −0.392 V for 1,3-DNB, −0.356 V for *o*-Cl, 0.0230 V for *o*-CHO, −0.913 V for *o*-COOH, −1.188 V for *o*-OH, −0.524 V for *o*-CH_3, ands −0.113 V for *m*-NO_2. Under the tested pH conditions (pH = 6.7), *o*-COOH ($pK_a = 1.43$) and *o*-OH ($pK_a = 4.09$) were completely dissociated to their anionic forms. This was considered in the calculation. The abbreviations *o*-COO^- and *o*-O^- were used hereafter to represent the ionized forms. It is worth noting that the temperature deviation of E^1_H calculation at standard state (25 °C) from batch kinetic experiments (35 °C) was equivalent for all tested NACs and should be cancelled in the regression.

2.6. Nitrogen kinetic isotope effects of 1,3-DNB reduction

The batch reaction of 1,3-DNB (initially at 13 μmol·L^{-1}) was conducted using the same method as described above with three different reductants: suspension of *B. subtilis* cells (2×10^{12} cells·L^{-1}), dissolved *B. subtilis* EPS (55.3 mgC·L^{-1}), and solution of sodium sulfide (5 mmol·L^{-1}, buffered with 50-mM Tris-HCl at pH 7.3). The residual 1,3-DNB after reaction at desired time intervals was extracted twice with trichloromethane at 1/1 ratio (v/v) by orbital shaking for 20 min at room temperature. The organic solvent was collected and filtered through anhydrous Na_2SO_4 (5 g) to remove water, and then evaporated to dryness under a steam of nitrogen. The residues were re-dissolved in 0.15-mL trichloroethane, and the nitrogen stable isotopes of 1,3-DNB were measured by a gas chromatography-combustion-isotope ratio mass spectrometer (GC-C-IRMS) (Thermo-Fisher, US) with a Thermo column. Helium was used as carrier gas at a flow rate of 1.0 mL·min^{-1}. The GC temperature program consisted of an initial oven temperature of 100 °C, held at 100 °C for 1 min, elevated from 100 to 200 °C at 20 °C·min^{-1} and then from 200 to 280 °C at 5 °C·min^{-1}, and finally held at 280 °C for 7 min. The $\delta^{15}N$ values of 1,3-DNB were derived from triplicate measurements with good precision (<0.5‰ and 1σ) and were reported relative to N_2 in air.

The bulk ^{15}N enrichment factor (ε_N) was determined from linear regression of Eq. (1) (Elsner et al., 2005; Hofstetter et al., 2008a).

$$\ln\left(\frac{\delta^{15}N+1}{\delta^{15}N_0+1}\right) = \varepsilon_N \ln\left(\frac{C}{C_0}\right) \quad (1)$$

where $\delta^{15}N_0$ and $\delta^{15}N$ are the ^{15}N signatures of the substrate at the start time and the given time of the reaction, respectively, and C_0 and C are the corresponding substrate concentrations. Apparent kinetic isotope effects of nitrogen, $AKIE_N$, were calculated according to Eq. (2) (Elsner et al., 2005; Hofstetter et al., 2008a).

$$AKIE_N = \left(\frac{1}{1+n/x \cdot z \cdot \varepsilon_N/1000}\right) \quad (2)$$

where n, x, and z are correction factors accounting for isotopic dilution (number of nitrogen isotope atoms), number of reactive sites, and number of reactive positions in intramolecular isotopic competition (Hartenbach et al., 2008; Hofstetter et al., 2008a). Thus, the overall correction factor ($n/x \cdot z$) for 1,3-DNB was equal to 2 accounting for isotopic dilution ($n = 2$), number of reactive sites ($x = 1$), and number of reactive positions ($z = 1$) in intramolecular isotopic competition (Hartenbach et al., 2008; Hofstetter et al., 2008a).

3. Results and discussion

3.1. Reduction of 1,3-DNB by bacterial cell suspension and EPS

Fig. 1a–b displays the residual ratio of 1,3-DNB, which is defined as the concentration of remaining 1,3-DNB at the end of the batch reaction to its initial concentration, for *B. subtilis* and *E. coli*, respectively. The transformation ratios of 1,3-DNB to 3-hydroxylaminonitrobenzene (intermediate) and 3-nitroaniline (product), which are defined as the concentrations of the newly formed compounds at the end of the reaction to the initial concentration of 1,3-DNB, are also presented in Fig. 1a–b. Summing up the three compounds results in a reasonable mass balance (78% for *B. subtilis* and 95% for *E. coli*). Nitroso derivatives and azo products likely accounted for the rest balance according to previous studies on NACs reduction (Kang and Zhu, 2013; Kulkarni and Chaudhari, 2007). Notably, 1,3-DNB, 3-hydroxylaminonitrobenzene, and 3-nitroaniline were only detected in the extracellular samples (supernatant and extracted EPS after reaction), but not in the intracellular samples or cell debris samples (detection limits about 0.4 μmol·L^{-1}). Thus, the reduction of 1,3-DNB occurred only in the extracellular matrix of the tested bacteria.

Both *B. subtilis* and *E. coli* could readily reduce 1,3-DNB. Approximately 73.2% of 1,3-DNB was reduced by pristine cells of *B. subtilis* after 10-h reaction, while 91.7% was reduced by pristine cells of *E. coli* after 3-h reaction. Clearly, *E. coli* cells were much more efficient than *B. subtilis* cells in 1,3-DNB reduction. For both *B. subtilis* and *E. coli*, the loss ratio of 1,3-DNB (calculated by one minus the residual ratio) increased with the addition of extra EPS (high-EPS cells). With the removal of EPS (low-EPS cells), the loss ratio of 1,3-DNB decreased for *E. coli*, but kept nearly constant for *B. subtilis*. However, the transformation ratio of 1,3-DNB to 3-nitroaniline (final reduction product) was much lower by low-EPS cells of *B. subtilis* (10.2%) than that by pristine cells of *B. subtilis* (17.6%), confirming that the reduction efficiency of 1,3-DNB in terms of the amount of electrons accepted was also lowered by the removal of EPS. With the exception of high-EPS cells of *B. subtilis*, the concentration of 3-hydroxylaminonitrobenzene far exceeded the concentration of 3-nitroaniline, especially for *E. coli* cells.

As shown in Fig. 1c–d, 1,3-DNB reduction was best described by the pseudo-first-order kinetic model ($R^2 > 0.96$). The observed pseudo-first-order kinetic rate constant (k_{obs}) was 0.136 ± 0.003 h^{-1} for pristine cells of *B. subtilis*, and 0.84 ± 0.09 h^{-1} for pristine cells of *E. coli* (see values in Table S1, Supporting Information). With the addition of extra EPS, the k_{obs} increased by 72.1% for *B. subtilis* cells and by 28.3% for *E. coli* cells. With removal of EPS, the k_{obs} decreased by 49.8% for *E. coli* cells, but by only 3.7% for *B. subtilis* cells. The loss ratio of 1,3-DNB by *E. coli* cells after knocking out the nitroreductase gene (Δ*nfsA*) is presented in Fig. 1b, and the reaction kinetics in Fig. 1d. Compared with the parent wild-type *E. coli* cells, 1,3-DNB reduction by the transformed cells was not impeded at all. Thus, the reduction of 1,3-DNB by the tested bacteria was not mediated by nitroreductases.

Fig. 2 displays the loss ratio and reaction kinetics of 1,3-DNB by different EPS (k_{obs} values summarized in Table S2). The reducing capability of EPS seemed to be much lower than that of bacterial cells. The loss ratio of 1,3-DNB was 80.7% for *E. coli* EPS after a 32-h reaction and 80.2% for *B. subtilis* EPS after a 42-h reaction (Fig. 2a). Consistent with the results of bacterial suspensions, *E. coli* EPS showed higher reducing capability than *B. subtilis* EPS (Fig. 2c). Moreover, the reducing capability of EPS extracted from *E. coli* cells was not decreased by knocking out the nitroreductase gene (Δ*nfsA*). The reducing capability was also compared between bulk *B. subtilis* EPS and the two molecular weight fractions, low-MW EPS (<3 kDa) and high-MW EPS (>3 kDa) (Fig. 2b and d). Adding the contributions of the two molecular weight fractions completely accounted for the overall loss ratio and reduction rate of 1,3-DNB by bulk *B. subtilis* EPS. However, the contributions of the two molecular weight fractions were not proportional to their TOC quotas (65% for low-MW EPS and 31% for high-MW EPS). In fact, >85% 1,3-DNB reduction was contributed by low-MW EPS, suggesting the predominant role played by the component. These observations rule out involvement of high-MW macromolecules such as proteins (cytochromes) in 1,3-DNB reduction by EPS.

3.2. Electron transfer characteristics of extracellular 1,3-DNB reduction

The nature of electron transfer in 1,3-DNB reduction by *B. subtilis* was examined by electrochemical cell analysis. As shown in Fig. 3a, *B. subtilis* cells and 1,3-DNB were individually placed in two flasks connected by a proton exchange membrane only to allow free proton exchange. Aliquots were withdrawn from the flask containing 1,3-DNB at desired time intervals to monitor the reaction. In the meantime, the quantity of electrons passing through the external circuit during the reaction was monitored. The stoichiometric demand of electrons in 1,3-DNB reduction was calculated by summing up the amounts of electrons needed to reduce 1,3-DNB to 3-nitroaniline (six electron equivalent) and to 3-hydroxylaminonitrobenzene (four electron equivalent). In principle,

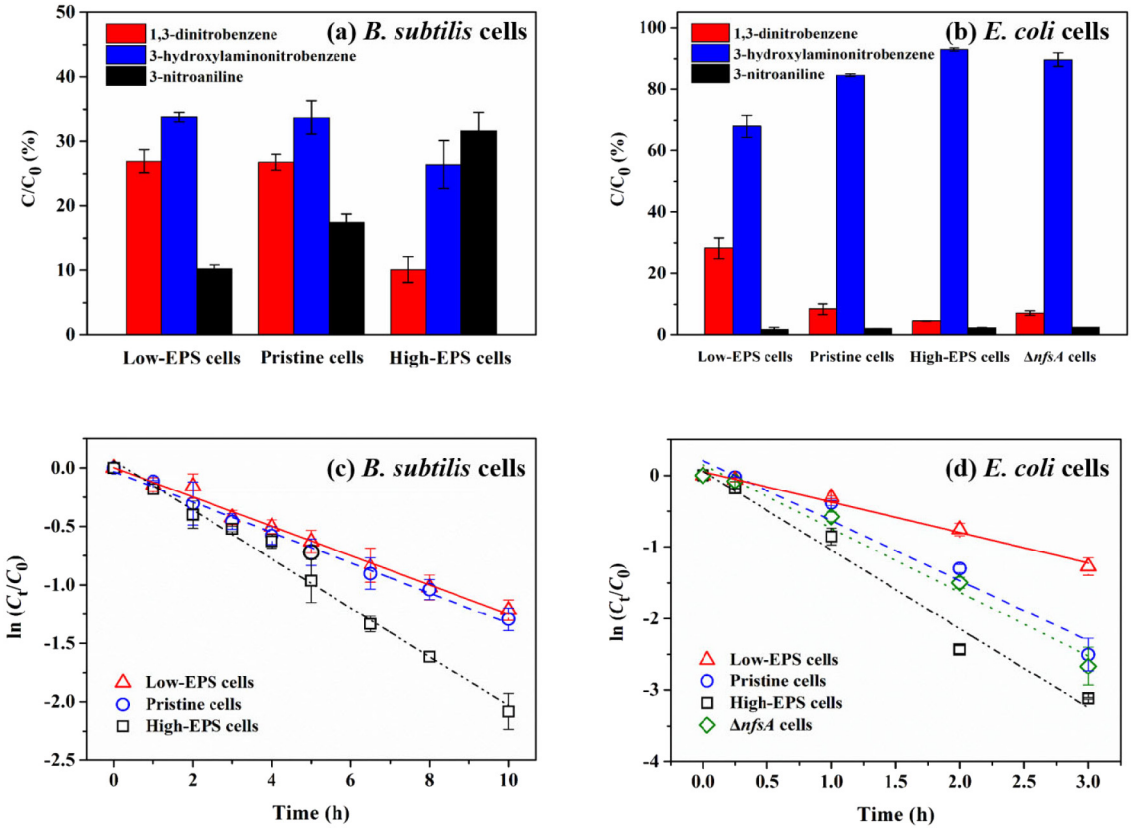

Fig. 1. Reduction of 1,3-dinitrobenzene in the presence of pristine cells without manipulation of EPS, low-EPS cells with removal of EPS by sonication/centrifugation, or high-EPS cells with addition of extra dissolved EPS for *B. subtilis* (2×10^{12} cells·L^{-1}) and *E. coli* (1.8×10^{12} cells·L^{-1}). (a), (b) Residual ratio of 1,3-dinitrobenzene (red bar), defined as the concentration of remaining 1,3-dinitrobenzene to its initial concentration (30 μmol·L^{-1} for *B. subtilis* and 40 μmol·L^{-1} for *E. coli*), and transformation ratios of 1,3-dinitrobenzene to 3-hydroxylaminonitrobenzene (blue bar) and 3-nitroaniline (black bar) at the end of the reaction for *B. subtilis* (a) and *E. coli* (b). (c), (d) Pseudo-first-order kinetics of 1,3-dinitrobenzene reduction plotted as ln (C_t/C_0) against time for *B. subtilis* (c) and *E. coli* (d). Error bars represent standard deviations calculated from triplicate samples. (For interpretation of the references to colour in this figure legend, the reader is referred to the web version of this article.)

the measured quantity of electron transfer through the external circuit was equal to the stoichiometric demand of electrons to reduce 1,3-DNB in the early stage (0–14 h) (Fig. 3b). However, at the end of the experiments (24 h), the measured quantity of electron transfer was nearly 50% higher than the stoichiometric demand of electrons to reduce 1,3-DNB. This was likely due to formation of unidentified reaction products in the late stage (Kang and Zhu, 2013) and/or electrode passivation. Nonetheless, the electrochemical analysis reaffirms that 1,3-DNB reduction occurred in the extracellular matrix and was not mediated by substrate-specific enzymes (e.g., nitroreductases).

Electron transfer mediators in the extracellular matrix involved in 1,3-DNB reduction were detected by fluorescence spectroscopy (Fig. 4). Flavins and quinone derivatives were found in extracellular supernatant and bulk EPS for both *B. subtilis* and *E. coli*, as reflected by the maximum emission wavelengths at 525 nm and 425 nm, respectively (Chen et al., 2003; Cory and Mcknight, 2005; Wang et al., 2013). Compared with the high-MW EPS, the low-MW EPS contained much higher contents of flavins and quinone derivatives. This was reasonable as the molecular weights of flavins and quinone derivatives generally fall within the range of several hundred Da (Light et al., 2018; Yang et al., 2016).

The extracellular electron transfer mediators were further probed by suppression experiments by 9.2-mM sodium azide (a cytochrome inhibitor) (Yang, 1985) and 0.1-mM rotenone (a NADH-ubiquinone reductase inhibitor) (Esposti, 1998) (Fig. 5a–b). For both *B. subtilis* ad *E. coli*, the presence of sodium azide suppressed 1,3-DNB reduction, with much more significant effects observed for *E. coli* cells (k_{obs} decreased by 89.2%, see Table S3), suggesting that cytochromes played an important role in the extracellular reduction of 1,3-DNB. Unlike *E. coli*, *B. subtilis* exhibited at least a 4-h lag in suppression reaction. Contrary to Gram-negative *E. coli* cells, Gram-positive *subtilis* cells have a much thicker cell wall (10 to 80 nm) and lack a periplasm for hosting large-quantity extracellular cytochromes, therefore resulting in delayed and weaker suppression effects. The presence of rotenone moderately suppressed 1,3-DNB reduction, wherein the k_{obs} decreased by 26.4% for *B. subtilis* and by 20.7% for *E. coli*. Thus, NADH-ubiquinone reductase participated in the extracellular reduction of 1,3-DNB. In contrast, the presence of rotenone caused no suppression effects on 1,3-DNB reduction by dissolved EPS extracted from *B. subtilis* (Fig. 5c), ruling out involvement of NADH-ubiquinone reductase. These results imply that electron transfer mediators involved in 1,3-DNB reduction might differ in type and efficiency between extracellular matrix and dissolved EPS. Additionally, the presence of 0.025-mM Au^{3+}, which depleted the reducing agents in EPS such as hemiacetals of reducing sugars (Kang et al., 2017), pronouncedly impeded 1,3-DNB reduction (k_{obs} decreased by 49.6%) (Fig. 5c), indicating the importance of these functionalities in 1,3-DNB reduction by EPS.

3.3. Structural dependence of the reduction of NACs

The structural dependence of reaction was examined with a total of seven NACs for both cells (2×10^{12} cells·L^{-1} for *B. subtilis* and 1.8×10^{12} cells·L^{-1} for *E. coli*) and both EPS (28.4 mgC·L^{-1} for *B. subtilis* EPS and 30.2 mgC·L^{-1} for *E. coli* EPS). The SAR was demonstrated by linear correlation between log k_{obs} (h^{-1}) and E^1_H (V) (Dunnivant et al., 1992;

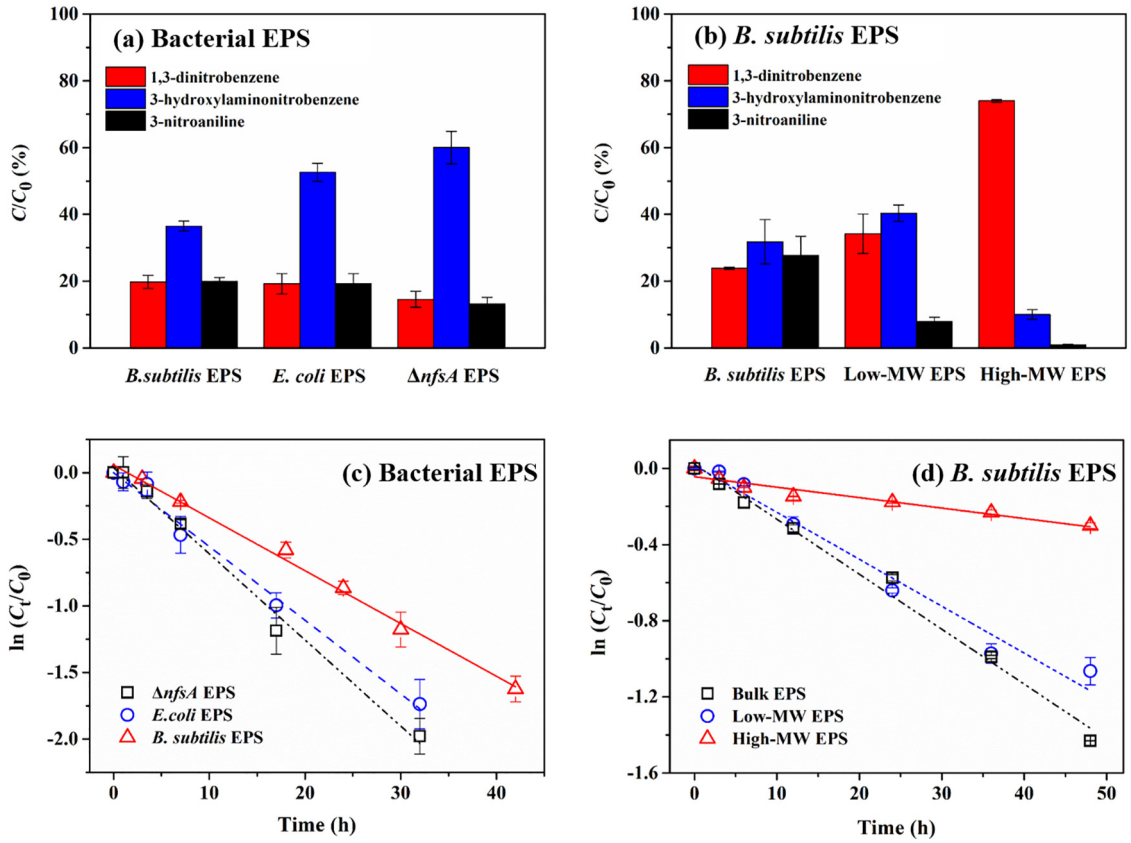

Fig. 2. Reduction of 1,3-dinitrobenzene in the presence of EPS (54.8 mgC·L^{-1}) separated from different microbes (*B. subtilis*, *E. coli*, and Δ*nfsA*) or different molecular weight fractions of *B. subtilis* EPS: bulk EPS (46.8 mgC·L^{-1}), low-MW EPS (30.4 mgC·L^{-1}), and high-MW EPS (14.5 mgC·L^{-1}). (a), (b) Residual ratio of 1,3-dinitrobenzene (red bar), defined as the concentration of remaining 1,3-dinitrobenzene to its initial concentration (13.0 μmol·L^{-1}), and transformation ratios of 1,3-dinitrobenzene to 3-hydroxylaminonitrobenzene (blue bar) and 3-nitroaniline (black bar) at the end of the reaction for EPS from different microbes (a) and *B. subtilis* EPS of different molecular weight fractions (b). (c), (d) Pseudo-first-order kinetics of reduction of 1,3-dinitrobenzene plotted as ln (C_t/C_0) against time for different EPS. Error bars represent standard deviations calculated from triplicate samples. (For interpretation of the references to colour in this figure legend, the reader is referred to the web version of this article.)

Schwarzenbach et al., 1990).

$$\log k_{obs} = \frac{aE_H^1}{2.303RT/F} + b \quad (3)$$

where slope a and intercept b are constant parameters, R is ideal gas constant (1/K), T is temperature (K), and F is Faraday's constant (C·mol^{-1}). The measured k_{obs} of the tested NACs varied by multiple orders of magnitude, ranging from 0.0016 ± 0.0004 h^{-1} (*o*-O$^-$) to 3.7 ± 0.9 h^{-1} (*o*-CHO) for *B. subtilis* and from 0.0013 ± 0.0005 (*o*-O$^-$) to 3.8 ± 0.3 h^{-1}(*o*-CHO) for *E. coli* (see values presented in Table S4). The k_{obs} increased with the electron-withdrawing ability of the substituted group in increasing order of *o*-O$^-$ < *o*-COO$^-$ < *o*-CH_3 < *o*-H (1,3-DNB) < *o*-Cl < *m*-NO_2 < *o*-CHO. Fig. 6 displays linear correlations between log k_{obs} and E_H^1 for bacterial cells and EPS. The strong linear correlation (R^2 > 0. 87) indicated that the rate-determining step for the reduction of NACs was the formation of free radicals of NACs by accepting one electron. Previous studies observed a similar k_{obs} versus E_H^1 relationship for the abiotic reduction of NACs by sulfides (Dunnivant et al., 1992; Schwarzenbach et al., 1990). The slopes (a)

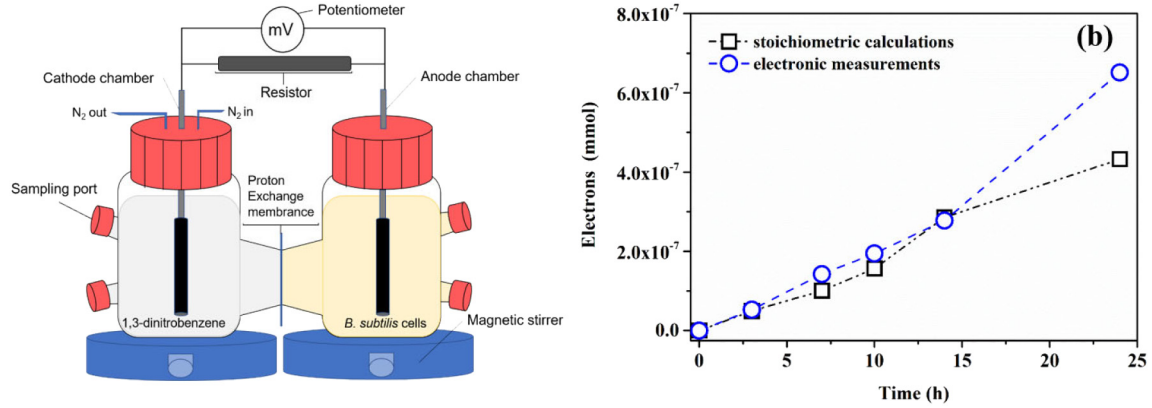

Fig. 3. Electrochemical cell analysis of 1,3-dinitrobenzene reduction by *B. subtilis* cells. (a) Schematic description of electrochemical cell set-up. (b) Comparison of electron transfer quantities in electrochemical cell experiment obtained by electronic measurements (open circles) and by stoichiometric calculations (open squares) based on the amounts of 1,3-dinitrobenzene reduced to 3-hydroxylaminonitrobenzene and 3-nitroaniline.

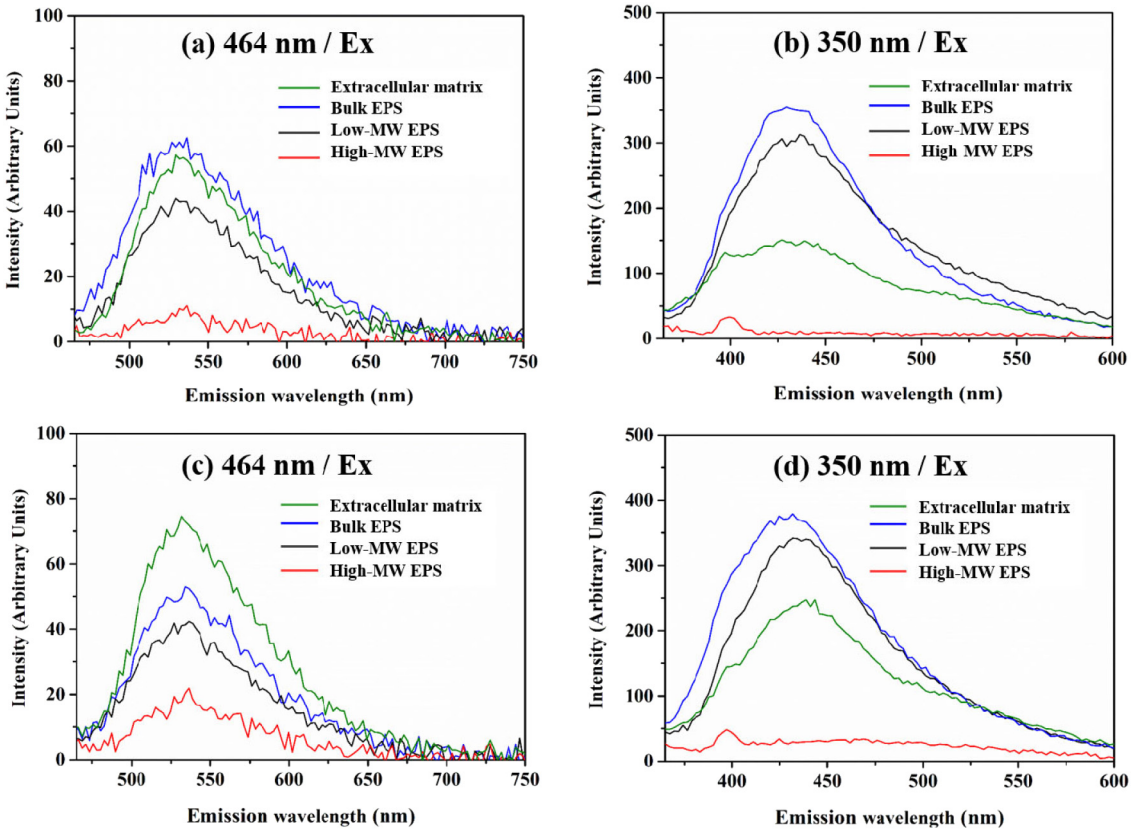

Fig. 4. Fluorescence emission spectra of microbial extracellular supernatant and different molecular weight fractions of EPS from *B. subtilis* (a, b) and *E. coli* (c, d) at given excitation (EX) wavelengths.

were 0.108 ± 0.008 (R^2 = 0.957) for *B. subtilis* cells, 0.096 ± 0.005 (R^2 = 0.872) for *B. subtilis* EPS, 0.117 ± 0.008 (R^2 = 0.904) for *E. coli* cells, and 0.101 ± 0.004 (R^2 = 0.956) for *E. coli* EPS. The much lower than unity slope values indicate that the overall reaction rate was only weakly dependent on the electron transfer between the terminal electron donor and NACs; however, the production of the terminal electron donors or the precursor formation was the rate-limiting step (Dunnivant et al., 1992). Furthermore, the very close slope values between bacterial cells and EPS indicated that they encountered the same rate-determining step in the reduction of NACs, which was likely to be the production of the terminal electron donors. Despite the very close slope values, the incept of the linear regression for bacterial cells was about one and half orders of magnitude higher than that for bacterial EPS, suggesting the much higher efficiency of bacterial cells in producing terminal electron donors under the experimental conditions.

3.4. Nitrogen kinetic isotope effects of 1,3-DNB reduction

Nitrogen kinetic isotope effects have been applied to differentiate physicochemical and biochemical reactions of NACs (Hartenbach et al., 2006; Hofstetter et al., 2008b; Wijker et al., 2017). The observable kinetic isotope effect of NACs, indexed by $AKIE_N$, can be lowered by the so called "masking effect" from non-fractionating steps (i.e., reversible binding to the active site of enzymes) preceding the actual nitrogen-oxygen bond cleavage (Hofstetter et al., 2008b; Wijker et al., 2017). For *B. subtilis* cells, *B. subtilis* EPS, and sodium sulfide, the ε_N, regression slope values in the plot of ($\delta^{15}N + 1000$) vs. ln (C_t/C_0), were determined to be −14 ± 2‰, −19.8 ± 0.4‰, and −20.9 ± 0.7‰, respectively (Fig. S2), and the $AKIE_N$ values were calculated to be 1.028 ± 0.004, 1.0413 ± 0.0008, and 1.044 ± 0.001. The values are summarized in Table S5, along with ε_N and $AKIE_N$ values for the reduction of NACs obtained from literature studies (Hartenbach et al., 2006; Hartenbach et al., 2008; Hofstetter et al., 2008b; Wijker et al., 2017). The $AKIE_N$ value for 1,3-DNB reduction by *B. subtilis* EPS was very close to that by sodium sulfide, suggesting the abiotic nature of the reaction with EPS. Consistently, the $AKIE_N$ value for the reduction of NACs (2- and 4-nitrotoluene) by 9,10-anthrahydroquinonone-2,6-disulfonate acid (AH_2QDS) was previously shown to range from 1.0396 to 1.0453 (Hartenbach et al., 2008). Compared with these abiotic reactions, the $AKIE_N$ value (1.028 ± 0.004) for 1,3-DNB reduction by *B. subtilis* cells was much lower, suggesting that other processes (i.e., reversible binding to extracellular active sites) might also contribute to the rate of reduction (Hofstetter et al., 2008b). In line with this observation, a previous study reported very similar $AKIE_N$ values from 1.0221 to 1.0273 for the reduction of NACs (nitrophenol and nitrobenzene) by *Pseudomonas* sp. under metabolism of electron-donor substrates (Hofstetter et al., 2008b; Wijker et al., 2017). Notably, introducing an electron transfer mediator into a redox system might affect the apparent kinetic isotope effect of the involved compound by facilitating the rate-limiting step. With the presence of juglone (a well-known electron transfer mediator), the $AKIE_N$ value for the reduction of NACs (2- and 4-chloronitrobenzenes) by sulfide ranged from 1.0288 to 1.0312 (Wijker et al., 2017), which was lower than the $AKIE_N$ value (1.043) observed herein for 1,3-DNB reduction by sulfide in the absence of any electron transfer mediator. Thus, the difference of $AKIE_N$ for 1,3-DNB reduction between *B. subtilis* cells and *B. subtilis* EPS could be due to the obviously more enriched and diversified electron transfer mediators in the extracellular matrix of living cells.

3.5. Mechanisms for extracellular reduction of NACs

We herein unambiguously demonstrate that two common bacteria, *B. subtilis and E. coli*, reduce 1,3-DNB within the extracellular matrix without involving any substrate-specific enzymes

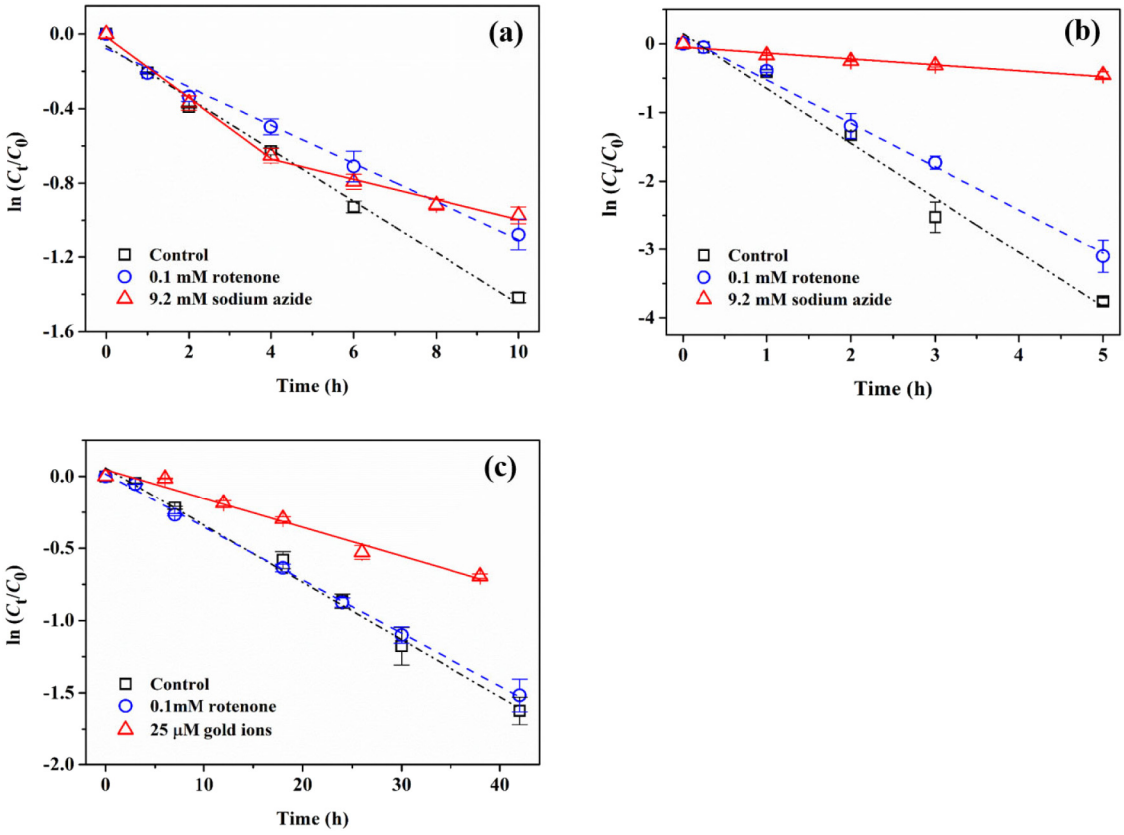

Fig. 5. Pseudo-first-order kinetics of 1,3-dinitrobenzene reduction plotted as ln (C_t/C_0) against time with and without the presence of different inhibitors (sodium azide, rotenone, and gold ions) for different systems. (a) *B. subtilis* (2×10^{12} cells·L^{-1}). (b) *E. coli* (1.8×10^{12} cells·L^{-1}). (c) *B. subtilis* EPS (56.9 mgC·L^{-1}). Error bars represent standard deviations calculated from triplicate samples.

(e.g., nitroreductases). Converging lines of evidence were obtained: 1) the parent compound (1,3-DNB), intermediate (3-hydroxylaminonitrobenzene), and product (3-nitroaniline) were only detected in the extracellular supernatant, but not within the tested cells; 2) knocking out nitroreductase *nfsA* gene caused no suppression effects on 1,3-DNB reduction by *E. coli* cells and *E. coli* EPS; 3) 1,3-DNB reduction could be successfully achieved by the electrochemical cell facility wherein bacterial cells and 1,3-DNB molecules were physically separated; 4) 1,3-DNB reduction could be induced by dissolved EPS alone, and the reaction was dominated by the low-MW EPS in which most enzymes (proteins) were excluded. To date most studies on extracellular reduction have focused on dissimilatory metal reduction (such as iron, manganese, and chromium) by electroactive bacteria including *Shewanella* sp. and *Geobacter* sp. (Marsili et al., 2008; Newman and Kolter, 2000; Shi et al., 2016). Only a few studies reported extracellular reduction of pentachlorophenol and azo-dyes by such bacteria mediated by exogenous electron transfer mediators (humin, 9,10-anthraquinone-2,6-disulfonate/AQDS) under anaerobic conditions (Pearce et al., 2010; Zhang and Katayama, 2012). The most remarkable finding of our study is that NACs could be effectively reduced in the extracellular matrix of common bacteria without involving any exogenous electron donors or electron transfer mediators, which are often scarce or limited under realistic environmental conditions.

Based on solid-state ^{13}C NMR analysis, we previously identified that the hemiacetal groups of reducing sugars and phenol groups in *E. coli* EPS were both involved in 1,3-DNB reduction (Kang and Zhu, 2013). Consistently, reduced juglone generated from electrochemical reduction according to literature method (Hartenbach et al., 2008) could

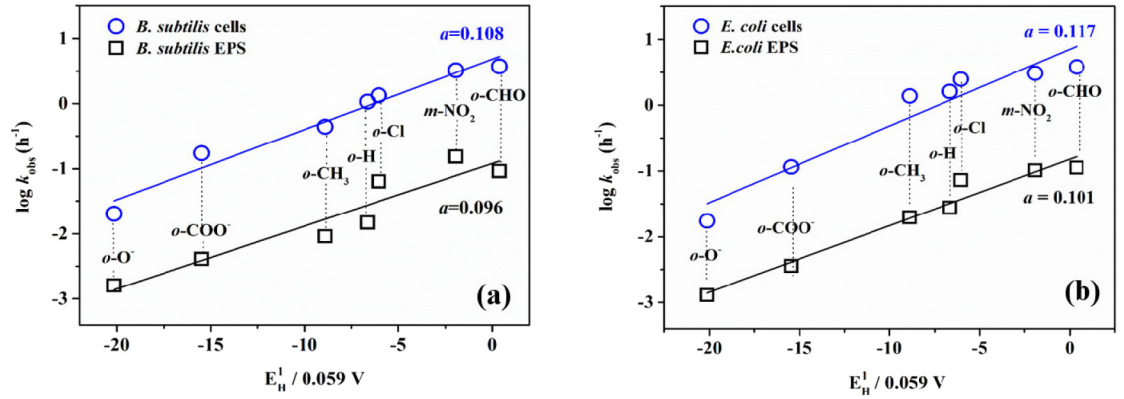

Fig. 6. Linear correlations between pseudo-first-order rate constants [log k_{obs} (h^{-1})] of reduction of various NACs and their one-electron reduction potentials [E^1_H/0.059 (V)] for *B. subtilis* (2×10^{12} cells·L^{-1}), *E. coli* (1.8×10^{12} cells·L^{-1}), *B. subtilis* EPS (28.4 mgC·L^{-1}), and *E. coli* EPS (30.3 mgC·L^{-1}). Regression slopes (a) are depicted.

readily reduce 1,3-DNB (Fig. S1a). Moreover, reduced riboflavin prepared using the same method could also reduce 1,3-DNB (Fig. S1b). However, glucose could not reduce 1,3-DNB even with the assistance of juglone or riboflavin as an electron shuttle (data not shown). Thus, the hydroquinone moieties (phenol group equivalents) as well as the reduced flavins in EPS likely acted as the terminal electron donors in 1,3-DNB reduction. In the absence of exogenous electron donors, bacterial cells consume hemiacetal groups of reducing sugars in EPS to generate electrons which are transferred through dissolved redox-active electron transfer mediators (flavins and quinones) to extracellular cytochromes and then to intracellular redox-active proteins (e.g., NADH-ubiquinone reductase). In fact, EPS can serve as surrogates of electron donors and probably carbon sources when these resources are scarce (Zhang and Bishop, 2003). Consistent with this hypothesis, removal of EPS (low-EPS cells) decreased the reduction efficiency of 1,3-DNB, whereas addition of extra EPS (high-EPS cells) increased the reduction efficiency of 1,3-DNB (Fig. 1). Additionally, the electron donors in EPS primarily comprised of the low molecular weight polysaccharides, hydroquinones, and reduced flavins, as demonstrated by the overwhelming reducing capability of the low-MW EPS relative to the high-MW EPS (Fig. 2b and d).

The minimal reduction suppression by rotenone (Fig. 5c) combined with the predominance of low-MW EPS in 1,3-DNB reduction (Fig. 2d) corroborated that redox-active/conductive proteins were not involved in the reduction of 1,3-DNB by EPS, reflecting the abiotic nature of the reaction. The abiotic nature of the reaction was also evidenced by the close $AKIE_N$ values observed between *B. subtilis* EPS and sodium sulfide (Table S5). On the other hand, the lack of redox-active/conductive proteins in dissolved EPS led to much lower reduction efficiency of 1,3-DNB compared to bacterial cells. Nonetheless, the nearly identical slope values obtained from the log k_{obs}-E_H^1 correlation relationship between *B. subtilis* cells and *B. subtilis* EPS (Fig. 6) strongly supported that they exploited the same primary electron donors to generate the same terminal electron donors (hydroquinones and reduced flavins) in NACs reduction.

4. Conclusions

This study investigated the underlying mechanisms for the extracellular reduction and electron transfer of two common bacteria, *B. subtilis* and *E. coli*, by comparing the characteristics of NACs reduction between bacterial cells and extracted dissolved EPS. Chemical, electrochemical, and biological analyses unambiguously demonstrate that NACs reduction occurs predominantly within the extracellular matrix. The hemiacetal groups of reducing sugars in EPS are proposed to be the primary electron donors, which further generate reduced electron transfer mediators (hydroquinones and reduced flavins) as the terminal electron donors to reduce NACs. Compared with extracted dissolved EPS, the EET by bacterial cells is much more efficient because of the presence of redox-active/conductive proteins (cytochromes and NADH-ubiquinone reductase). These results demonstrate that EET can be exploited by non-electroactive, common bacteria (*B. subtilis* and *E. coli*) in the absence of exogenous electron donors to reduce organic compounds. Overall, these findings advance fundamental understanding of microbial extracellular reduction of high-oxidation-state pollutants (such as NACs, chromate, and perchlorate), not only for environmental fate assessment but also for informing the development of bioremediation technologies.

CRediT authorship contribution statement

Dongqiang Zhu provided the original idea and prepared the paper with contributions from all co-authors. **Xinwei Zhou** designed and conducted the research. **Fuxing Kang**, **Xiaolei Qu**, **Heyun Fu**, and **Juan Liu** were involved in the development of the analysis methods. **Pedro J. Alvarez** reviewed the written document.

Declaration of competing interest

The authors declare that they have no known competing financial interests or personal relationships that could have appeared to influence the work reported in this paper.

Acknowledgments

This work was supported by the National Natural Science Foundation of China (Grants 21920102002, 21777002, and 41991331).

Appendix A. Supplementary data

The k_{obs} values for NACs reduction in different reaction systems can be found in Tables S1–S4 in Supporting Information. Table S5 compares nitrogen kinetic isotope effects for 1,3-DNB reduction and data for NACs reduction collected from literature studies. Fig. S1 displays reduction kinetics of 1,3-DNB by electrochemically reduced juglone and riboflavin. Fig. S2 displays bulk ^{15}N enrichment factors in 1,3-DNB reduction for different reaction systems. Supplementary data to this article can be found online at https://doi.org/10.1016/j.scitotenv.2020.138291.

References

Aruoja, V., Sihtmäe, M., Dubourguier, H.C., Kahru, A., 2011. Toxicity of 58 substituted anilines and phenols to algae *Pseudokirchneriella subcapitata* and bacteria *Vibrio fischeri*: comparison with published data and QSARs. Chemosphere 84, 1310–1320.
Boggs, M.A., Jiao, Y., Dai, Z., Zavarin, M., Kersting, A.B., 2016. Interactions of Plutonium with *Pseudomonas* sp. EPS-1W and its extracellular polymeric substances. Appl. Environ. Microbiol. 82, 7093–7101.
Borole, A.P., Reguera, G., Ringeisen, B., Wang, Z.W., Feng, Y., Kim, B.H., 2011. Electroactive biofilms: current status and future research needs. Energy Environ. Sci. 4, 4813–4834.
Carlson, H.K., Iavarone, A.T., Gorur, A., Yeo, B.S., Tran, R., Melnyk, R.A., Mathies, R.A., Auer, M., Coates, J.D., 2012. Surface multiheme *c*-type cytochromes from *Thermincola potens* and implications for respiratory metal reduction by gram-positive bacteria. Proc. Natl. Acad. Sci. U. S. A. 109, 1702–1707.
Chen, W., Westerhoff, P., Leenheer, J.A., Booksh, K., 2003. Fluorescence excitation–emission matrix regional integration to quantify spectra for dissolved organic matter. Environ. Sci. Technol. 37, 5701–5710.
Cory, R.M., Mcknight, D.M., 2005. Fluorescence spectroscopy reveals ubiquitous presence of oxidized and reduced quinones in dissolved organic matter. Environ. Sci. Technol. 39, 8142–8149.
Dunnivant, F.M., Schwarzenbach, R.P., Macalady, D.L., 1992. Reduction of substituted nitrobenzenes in aqueous solutions containing natural organic matter. Environ. Sci. Technol. 26, 2133–2141.
Elsner, M., Zwank, L., Hunkeler, D., Schwarzenbach, R.P., 2005. A new concept linking observable stable isotope fractionation to transformation pathways of organic pollutants. Environ. Sci. Technol. 39, 6896–6916.
Esposti, M.D., 1998. Inhibitors of NADH-ubiquinone reductase: an overview. BBA-Bioenergetics 1364, 222–235.
Flemming, H., Wingender, J., 2010. The biofilm matrix. Nat. Rev. Microbiol. 8, 623–633.
Gorontzy, T., Küver, J., Blotevogel, K.H., 1993. Microbial transformation of nitroaromatic compounds under anaerobic conditions. J. Gen. Microbiol. 139, 1331–1336.
Gralnick, J.A., Newman, D.K., 2007. Extracellular respiration. Mol. Microbiol. 65, 1–11.
Hartenbach, A.E., Hofstetter, T.B., Berg, M., Bolotin, J., Schwarzenbach, R.P., 2006. Using nitrogen isotope fractionation to assess abiotic reduction of nitroaromatic compounds. Environ. Sci. Technol. 40, 7710–7716.
Hartenbach, A.E., Hofstetter, T.B., Aeschbacher, M., Sander, M., Kim, D., Strathmann, T.J., Arnold, W.A., Cramer, C.J., Schwarzenbach, R.P., 2008. Variability of nitrogen isotope fractionation during the reduction of nitroaromatic compounds with dissolved reductants. Environ. Sci. Technol. 42, 8352–8359.
Hofstetter, T.B., Neumann, A., Arnold, W.A., Hartenbach, A.E., Bolotin, J., Cramer, C.J., Schwarzenbach, R.P., 2008a. Substituent effects on nitrogen isotope fractionation during abiotic reduction of nitroaromatic compounds. Environ. Sci. Technol. 42, 1997–2003.
Hofstetter, T.B., Spain, J.C., Nishino, S.F., Bolotin, J., Schwarzenbach, R.P., 2008b. Identifying competing aerobic nitrobenzene biodegradation pathways by compound-specific isotope analysis. Environ. Sci. Technol. 42, 4764–4770.
Kang, F.X., Zhu, D.Q., 2013. Abiotic reduction of 1,3-DNB by aqueous dissolved extracellular polymeric substances produced by microorganisms. J. Environ. Qual. 42, 1441–1448.
Kang, F.X., Alvarez, P.J., Zhu, D.Q., 2014. Microbial extracellular polymeric substances reduce Ag+ to silver nanoparticles and antagonize bactericidal activity. Environ. Sci. Technol. 48, 316–322.
Kang, F.X., Qu, X., Alvarez, P.J., Zhu, D.Q., 2017. Extracellular saccharide-mediated reduction of Au^{3+} to gold nanoparticles: new insights for heavy metals biomineralization on microbial surfaces. Environ. Sci. Technol. 51, 2776–2785.
Kulkarni, M., Chaudhari, A., 2007. Microbial remediation of nitro-aromatic compounds: an overview. J. Environ. Manag. 85, 496–512.

Li, S.W., Sheng, G.P., Cheng, Y.Y., Yu, H.Q., 2016. Redox properties of extracellular polymeric substances (EPS) from electroactive bacteria. Sci. Rep. 6, 39098.
Light, S.H., Su, L., Rivera-Lugo, R., Cornejo, J.A., Louie, A., Iavarone, A.T., Ajo-Franklin, C.M., Portnoy, D.A., 2018. A flavin-based extracellular electron transfer mechanism in diverse gram-positive bacteria. Nature 562, 140–144.
Lovley, D.R., 2006. Bug juice: harvesting electricity with microorganisms. Nat. Rev. Microbiol. 4, 497–508.
Lovley, D.R., 2008. Extracellular electron transfer: wires, capacitors, iron lungs, and more. Geobiology 6, 225–231.
Marsili, E., Baron, D.B., Shikhare, I.D., Coursolle, D., Gralnick, J.A., Bond, D.R., 2008. *Shewanella* secretes flavins that mediate extracellular electron transfer. Proc. Natl. Acad. Sci. U. S. A. 105, 3968–3973.
Marvin-Sikkema, F.D., Bont, J.A.M.D., 1994. Degradation of nitroaromatic compounds by microorganisms. Appl. Microbiol. Biotechnol. 42, 499–507.
Newman, D.K., Kolter, R., 2000. A role for excreted quinones in extracellular electron transfer. Nature 405, 94–97.
Pearce, C.I., Christie, R., Boothman, C., Canstein, H.V., Guthrie, J.T., Lloyd, J.R., 2010. Reactive azo dye reduction by *Shewanella* strain J18 143. Biotechnol. Bioeng. 95, 692–703.
Phillips, K.L., Sandler, S.I., Chiu, P.C., 2008. A method to calculate the one-electron reduction potentials for nitroaromatic compounds based on gas-phase quantum mechanics. J. Comput. Chem. 32, 226–239.
Reguera, G., Nevin, K.P., Nicoll, J.S., Covalla, S.F., Woodard, T.L., Lovley, D.R., 2006. Biofilm and nanowire production leads to increased current in *Geobacter sulfurreducens* fuel cells. Appl. Environ. Microbiol. 72, 7345–7348.
Roldán, M.D., Pérez-Reinado, E., Castillo, F., Moreno-Vivián, C., 2010. Reduction of polynitroaromatic compounds: the bacterial nitroreductases. FEMS Microbiol. Rev. 32, 474–500.
Salter-Blanc, A.J., Bylaska, E.J., Johnston, H.J., Tratnyek, P.G., 2015. Predicting reduction rates of energetic nitroaromatic compounds using calculated one-electron reduction potentials. Environ. Sci. Technol. 49, 3778–3786.
Schwarzenbach, R.P., Stierli, R., Lanz, K., Zeyer, J., 1990. Quinone and iron porphyrin mediated reduction of nitroaromatic compounds in homogeneous aqueous solution. Environ. Sci. Technol. 24, 1566–1574.
Shi, L., Dong, H.L., Reguera, G., Beyenal, H., Lu, A.H., Liu, J., Yu, H., Fredrickson, J.K., 2016. Extracellular electron transfer mechanisms between microorganisms and minerals. Nat. Rev. Microbiol. 14, 651–662.
Somerville, C.C., Nishino, S.F., Spain, J.C., 1995. Purification and characterization of nitrobenzene nitroreductase from *Pseudomonas pseudoalcaligenes* JS45. J. Bacteriol. 177, 3837–3842.
Spain, J.C., 1995. Biodegradation of nitroaromatic compounds. Annu. Rev. Microbiol. 49, 523–555.
Vu, B., Chen, M., Crawford, R.J., Ivanova, E.P., 2009. Bacterial extracellular polysaccharides involved in biofilm formation. Molecules 14, 2535–2554.
Wang, J., Lu, H., Zhou, Y., Song, Y., Liu, G., Feng, Y., 2013. Enhanced biotransformation of nitrobenzene by the synergies of *Shewanella* species and mediator-functionalized polyurethane foam. J. Hazard. Mater. 252–253, 227–232.
Wijker, R.S., Zeyer, J., Hofstetter, T.B., 2017. Isotope fractionation associated with the simultaneous biodegradation of multiple nitrophenol isomers by *Pseudomonas putida* B2. Environ. Sci.: Processes Impacts 19, 775–784.
Xiao, Y., Zhang, E., Zhang, J., Dai, Y., Yang, Z., Christensen, H.E.M., Ulstrup, J., Zhao, F., 2017. Extracellular polymeric substances are transient media for microbial extracellular electron transfer. Sci. Adv. 3, e1700623.
Xiong, Y., Shi, L., Chen, B., Mayer, M.U., Lower, B.H., Londer, Y., Bose, S., Hochella, M.F., Fredrickson, J.K., Squier, T.C., 2006. High-affinity binding and direct electron transfer to solid metals by the *Shewanella oneidensis* MR-1 outer membrane *c*-type cytochrome OmcA. J. Am. Chem. Soc. 128, 13978–13979.
Yang, T., 1985. Mechanism of nitrite inhibition of cellular respiration in *Pseudomonas aeruginosa*. Curr. Microbiol. 12, 35–39.
Yang, Z., Kappler, A., Jiang, J., 2016. Reducing capacities and distribution of redox-active functional groups in low molecular weight fractions of humic acids. Environ. Sci. Technol. 50, 12105–12113.
Yuan, X., Lu, G., Lang, P., 1997. QSAR study of the toxicity of nitrobenzenes to river bacteria and *Photobacterium phosphoreum*. Bull. Environ. Contam. Toxicol. 58, 123–127.
Zhang, X., Bishop, P.L., 2003. Biodegradability of biofilm extracellular polymeric substances. Chemosphere 50, 63–69.
Zhang, C., Katayama, A., 2012. Humin as an electron mediator for microbial reductive dehalogenation. Environ. Sci. Technol. 46, 6575–6583.